STATICAL BEHAVIOUR OF LONG-SPAN CABLE-STAYED BRIDGES

M. COMO

Istituto di Tecnica delle Costruzioni, Facoltà di Ingegneria, Piazzale Tecchio, Napoli, Italia

and

A. GRIMALDI AND F. MACERI

Facoltà di Ingegneria, Seconda Università di Roma, Via Orazio Raimondo, 00173 Roma, Italia

Abstract—The aim of this study is to examine the statical behaviour of the long-span cable-stayed bridge with fan scheme by means of a suitable continuous model.

The given solution of the Statics basic equations of the model focalizes a prevailing truss behaviour of the bridge.

This solution in fact–developed according to the perturbative technique–gives as the generating term the "truss solution" of the bridge and, as correction terms–of higher order in the perturbative parameter–the local bending effects on the girder.

According to this solution it is possible to achieve a synthetic understanding of the statical behaviour of the bridge and to express, by simple formulas, the more interesting required quantities.

The obtained results are checked with some numerical solutions obtained via finite element methods that confirm the soundness of the proposed model.

NOTATION

a stay's nondimensional deformability
$A_s(A_0)$ stay (anchor stay) cross-sectional area
$\alpha(\alpha_0)$ stay (anchor stay)-girder angle
$\beta(\beta_0)$ stay's (anchor stay's) stress ratio
C_t girder torsional stiffness
δ midspan deflection
Δ stay's spacing
$\Delta\epsilon_s^*$ fictitious deformation increment
$\Delta\sigma$ stress increment
E elasticity (Young's) modulus
E_s^* Dishinger's fictitious elasticity modulus
ϵ strain; also, girder nondimensional stiffness
g dead load
γ specific weight
H tower height
I girder inertia
K tower stiffness
l lateral span length
l_0 cable horizontal projection's length
L central span length
λ flexural displacement wavelength
$m_s(m_t)$ torsional action of the stays (torsional load) on the girder
M bending moment in the girder
M_t twisting moment in the girder
μ nondimensional torsional load
n distributed axial force along the stay's curtain
N axial force in the girder
$N_0(N_s)$ axial force in the (anchor) stay
p live load
P nondimensional live load
$q_0(q_v)$ horizontal (vertical) component of the load q
$R_p(R_s)$ pile (side support) vertical reaction
ρ nondimensional cable curtain stiffness
S_0 horizontal component of the anchor cable's axial force
σ stress
σ_a allowable stress
$\sigma_g(\sigma_p)$ stress produced in the stays by dead (live) load
σ_g^0 stress produced in the anchor stay by dead load

σ_1, σ_2 initial and final stress values in a stay
r_1, r_2 geometrical aspect ratios of the bridge
ϑ girder torsional angle
τ girder nondimensional torsional stiffness
$\vartheta_0(\vartheta_1)$ truss-like (flexural) part of ϑ
u, v, w displacement parameters of the bridge
U, V, W nondimensional displacement parameters
U_0, V_0, W_0
(U_1, V_1, W_1) truss-like (flexural) part of U, V, W
x, y, z coordinates
ζ nondimensional abscissa
φ stay distribution function
$\chi(\chi_0)$ nondimensional tower (anchor cable) stiffness
$\Psi_R(\Psi_L)$ right (left) pylon torsional rotation
$\Psi_0(\Psi_1)$ truss-like (torsional) part of Ψ

1. INTRODUCTION

In the second half of this century the cable-stayed bridge has found a successful renewal. Particularly, in the last decade, the fan-shaped truss-like scheme obtained a special interest as a valid alternative solution for long spans, compared with the suspension bridge[1–6].

The physical behaviour of the fan-shaped scheme (Fig. 1) is very similar to that of a large truss structure where the main state of stress is given by axial forces in the stays and in the girder, while girder bending is of secondary importance.

This scheme most conveniently applies when spans are more than 300 m long. In such instances, the spacing between stays is usually small compared to the bridge's main span and we may therefore reasonably suppose a continuous stay distribution along the deck, for the purpose of an analytical investigation[7].

In this article the static behaviour of long-span cable-stayed bridges is studied by means of a continuous model.

The fundamental assumptions of the analysis are:
(i) diffused stay arrangement along the deck;
(ii) truss-like statical scheme.

By the first condition, the analytical problem is decribed by a convenient set of integro-differential equations. An approximate solution of these equations can be given which analytically reflects the second assumption, namely that of the state of axial forces prevailing over the flexural one.

Within this framework, it is possible to develop a simple analysis of the long-span cable-stayed bridge, which, though approximated, collects main qualitative and quantitative aspects and translates them into simple results. Finally, it is shown that the continuous model results agree satisfactorily with some numerical computations corresponding to the usual discrete model of the bridge.

2. STATICAL BEHAVIOUR: PRELIMINARY ASSUMPTIONS

The statical scheme we shall examine (Fig. 1) is characterized by the following parameters:

H = tower height;
L = central span length;
l = lateral span length;
Δ = stays spacing;
α = stay-girder angle;
A_s = stay cross-sectional area;
A_0 = anchor stay cross-sectional area;
I = girder inertia;
K = tower stiffness.

It is known[4] that, in order for the anchor cable to be stable, the ratio L/l should not be any smaller than ~2.8, while the ratio H/L is usually set at 0.2, which is the
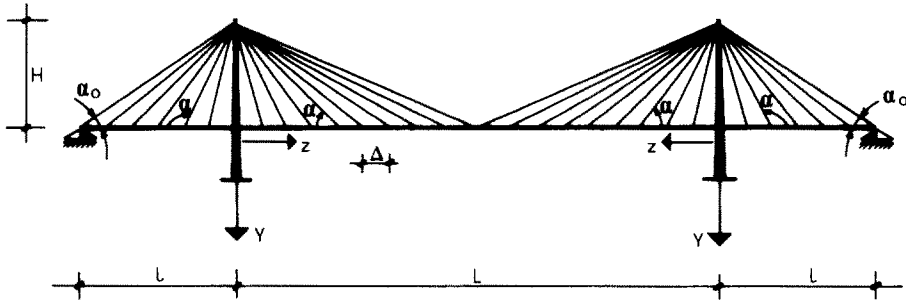
Fig. 1. Structural scheme of the bridge.

optimum value referred to the cable's weight. In the numerical examples, values of $L/l = 3$ and $H/L = 0.2$ were therefore used. The constraints are shown in Fig. 1: the girder is supposed to be not horizontally constrained with respect to statical forces, while damping devices take care of dynamic actions (braking, etc.).

The statical analysis of the bridge has to be performed in different ways according to where live p or dead g loads are considered.

Stresses produced by dead loads are strictly dependent on the erection procedure of the bridge. Decks are usually cantilever erected; in this case tensions may be so controlled in stays that the deck's final configuration is straight and free from bending moments. Stresses produced by dead loads g are evaluated from the statically determinate scheme where hinges are placed at the nodes[4, 5, 6].

Let N be the axial force in the girder, N_s the force in a generical stay and $n = N_s/\Delta$ the axial force distributed along the continuous curtain of stays. From the condition of equilibrium of the girder we immediately get

$$n(\zeta) = g(1 + \zeta^2)^{1/2} \tag{1}$$

$$N(\zeta) = g\frac{H}{2}\left[\left(\frac{L}{2H}\right)^2 - \zeta^2\right] \tag{2}$$

where ζ is the adimensional abscissa along the girder (Fig. 1):

$$\zeta = \frac{z}{H}. \tag{3}$$

The axial force N_0 in the anchor stay is

$$N_0 = \frac{gl}{2}\left[1 + \left(\frac{l}{H}\right)^2\right]\left[\left(\frac{L}{2l}\right)^2 - 1\right] \tag{4}$$

and the reactions R_s of the side supports and R_p of the piles are:

$$R_s = \frac{gl}{2}\left[\left(\frac{L}{2l}\right)^2 - 1\right] \tag{5}$$

$$R_p = \frac{gl}{2}\left[\frac{L}{2l} + 1\right]^2. \tag{6}$$

As far as the effects of live loads p are concerned, the prevailing behaviour is still truss like. In the girder, in fact, as shown in the next sections, there are also bending stresses that, for long spans, have only local character and are weakly dependent on the span length.

While the axial stresses can be evaluated according to the truss scheme, bending stresses in the girder depend on the relative stay-girder stiffness. To evaluate defor-

mations or stresses in the girder, it is very important to evaluate first the elastic response of the single stay, already in tension for dead loads, to a generic deformation increment $\Delta\epsilon_s^*$. The Dischinger modulus, as it is well known, can characterize this tangent response of the single stay[1].

The stay axial force increment can, in fact, be evaluated as

$$\Delta N_s = E_s^* \Delta \epsilon_s^* A_s \tag{7}$$

where E_s^*, the Dischinger fictitious elasticity modulus, is a function of the primitive dead load tension in the stay:

$$E_s^* = \frac{E}{1 + \dfrac{E\gamma^2 l_0^2}{12\sigma_1^3}} \tag{8}$$

with E the Young modulus, γ the specific weight and l_0 the horizontal projection of the stay length (Fig. 3).

The tangent Dischinger modulus (8) gives a sufficient approximation if the initial stress σ_1 is not too low and the stress increment $\Delta\sigma$ is small.

It is, on the other hand, possible to obtain a more accurate evaluation of the stay response by using the secant Dischinger modulus:

$$E_s^* = \frac{E}{1 + \left(\dfrac{E\gamma^2 l_0^2}{12\sigma_1^3}\right)\left(\dfrac{1+\beta}{2\beta^2}\right)} \tag{9}$$

where β represents the ratio between the final value of the stay tension σ_2, and the initial one σ_1. The secant modulus approximation requires an estimate of the final stress σ_2.

3. CONTINUOUS-MODEL EQUATIONS

Deformations and stresses produced by live loads can be evaluated by analyzing the linearized response of the bridge starting from the dead loads equilibrium configuration. The reactivity of previously existing axial forces in stays to further deformations are defined through Dischinger's fictitious elasticity modulus.

Vertical loads, symmetrically placed with respect to the bridge's longitudinal symmetry plane, will be considered first.

Next, torsional effects produced by load eccentricities will be studied.

3.1 In-plane analysis

The girder and pylon's extensional deformability can usually be neglected.

The bridge's additional deformation, when no torsion occurs, is then determined by the following displacement parameters (Fig. 2):

(i) the girder's vertical displacements $v(z)$;
(ii) the girder's horizontal displacement w;
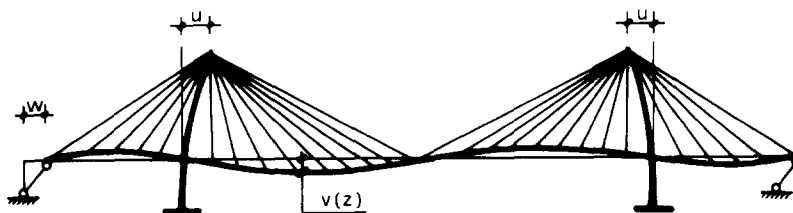(iii) the pylon tops' horizontal displacement u.

Fig. 2. Bridge deformation and displacement parameters.

As already said, the bridge's structure is symmetrical, the pylons are not joined with the girder which has no statical horizontal constraints. Consequently, the horizontal equilibrium of the bridge's left and right sides requires shear forces to be the same at the pylon tops sections.

Therefore, however vertical loads are placed on the deck, displacements of the pylon tops will always be opposite. This is why one parameter has been employed for the pylon displacements.

The effect of live loads may be analyzed only after examining the behaviour of a single stay when the previously defined u, v, w bridge displacements occur. Let us refer to a generic stay anchored to the left tower (Fig. 3). The $\Delta\epsilon_s^*$ deformation increment produced by u, v, w displacements is

$$\Delta\epsilon_s^* = \frac{\Delta l_s}{l_s} = (v \sin \alpha + (w - u) \cos \alpha)\frac{1}{l_s}$$

$$= \frac{v}{H} \sin^2 \alpha + \frac{w - u}{H} \sin \alpha \cos \alpha. \tag{10}$$

The stay axial force increment ΔN_s is then evaluated by eqns (7) and (10). The horizontal ΔN_s^0 and vertical ΔN_s^v components of ΔN_s are the contributions of the stay's axial deformation to the new actions produced on the girder:

$$\Delta N_s^v = -\frac{v}{H} E_s^* A_s \sin^3 \alpha + \frac{u \pm w}{H} E_s^* A_s \sin^2 \alpha \cos \alpha \tag{11}$$

$$\Delta N_s^0 = \pm \frac{v}{H} E_s^* A_s \sin^2 \alpha \cos \alpha - \frac{w \pm u}{H} E_s^* A_s \sin \alpha \cos^2 \alpha \tag{11'}$$

where the $-$ or $+$ sign applies to the left or right pylon, respectively. Furthermore, relations (11) represent the action of stays on the girder with signs in agreement with the axes of Fig. 1.

The sections A_s and A_0 are found from the design values σ_g and σ_g^0 of the stays tension due to dead loads of the continuous stays curtain and of the anchor cable, respectively. We have:

$$A_s = \frac{g\Delta}{\sigma_g \sin \alpha} \tag{12}$$

$$A_0 = \frac{gl}{2\sigma_g^0}\left[1 + \left(\frac{l}{H}\right)^2\right]^{1/2}\left[\left(\frac{L}{2l}\right)^2 - 1\right]. \tag{13}$$

According to the assumption of uniform stay distribution, we finally get the following vertical and horizontal forces per unit length on the girder:

$$q_v = \frac{E_s^* A_s}{H\Delta}\left[-v \sin^3 \alpha + (u \pm w) \sin^2 \alpha \cos \alpha\right] \tag{14}$$

$$q_0 = \frac{E_s^* A_s}{H\Delta}\left[\pm v \sin^2 \alpha \cos \alpha - (\pm u + w) \sin \alpha \cos^2 \alpha\right]. \tag{15}$$
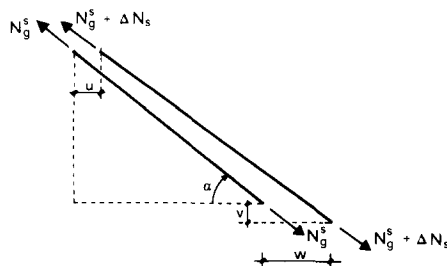

Fig. 3. Strain and stress in the deformed stay.

Equations (14) and (15) characterize the interaction between the stays and girder, thus enabling us to write the bridge's equilibrium equations in terms of the three displacement parameters u, v, w.

In fact, we get

Flexural girder equilibrium

The girder equilibrium equation, neglecting the effect of the axial stress produced by dead load, is

$$EIv^{IV} = q_v + p \tag{16}$$

where $p(z)$ is the live load.

The other two equations should express the equilibrium conditions corresponding to the relative displacement u between pylons, and to the girder's horizontal translation w. The following equations are found to be equivalent to the former (Fig. 4):

Left pylon equilibrium

$$\int_L (-q_0)\,dz - Ku - S_0 = 0 \tag{17}$$

Right pylon equilibrium

$$\int_R (-q_0)\,dz + Ku - S_0 = 0. \tag{18}$$

In eqns (17) and (18) q_0 is given by (15) and the integration is extended to the stays curtain belonging to the bridge's left or right side, respectively; K is the pylon tops' flexural stiffness and S_0 is the horizontal component of the anchor cable's axial force:

$$S_0 = -(w \mp u)\frac{E_0^* A_0}{H}\sin \alpha_0 \cos^2 \alpha_0 \tag{19}$$

where the $-$ or $+$ sign applies to the left- or right-hand anchor stay, respectively.

Inserting (14) and (15) into (16), (17) and (18) we get

Girder equilibrium

$$EIv^{IV} + \frac{E_s^* A_s}{H\Delta}\sin^3 \alpha \qquad v - \frac{E_s^* A_s}{H\Delta}(u \mp w)\sin^2 \alpha \cos \alpha = p \tag{20}$$

Left pylon equilibrium

$$A_1 w - A_2 u + \int_L \frac{E_s^* A_s}{H\Delta}\sin^2 \alpha \cos \alpha\, v\,dz = 0 \tag{21}$$

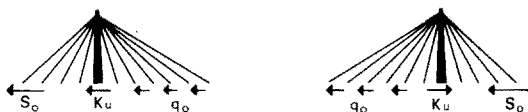Fig. 4. Horizontal forces on the pylon tops.

Right pylon equilibrium

$$A_1 w + A_2 u - \int_R \frac{E_s^* A_s}{H\Delta} \sin^2 \alpha \cos \alpha \, v \, dz = 0 \tag{22}$$

where

$$A_1 = \int_L \frac{E_s^* A_s}{H\Delta} \sin \alpha \cos^2 \alpha \, dz + \frac{E_0 A_0}{H} \sin \alpha_0 \cos^2 \alpha_0 \tag{23}$$

$$A_2 = A_1 + K. \tag{24}$$

Equations (20), (21), and (22) should be conveniently made dimensionless. Therefore, let

$$V = \frac{v}{H} \qquad U = \frac{u}{H} \qquad W = \frac{w}{H}, \tag{25}$$

and from here onwards

$$(\ )' = \frac{d(\ )}{d\zeta} \tag{25'}$$

will denote derivatives with respect to the dimensionless abscissa ζ.
   Equation (20) becomes

$$\frac{EI}{H^3} V^{IV} + \frac{E_s^* A_s}{\Delta} \sin^3 \alpha \, V - \frac{E_s^* A_s}{\Delta} (U \mp W) \sin^2 \alpha \cos \alpha = p. \tag{26}$$

It should also be noted that

$$\frac{E_s^* A_s}{E\Delta} = \frac{1}{1 + a\zeta^2} \frac{g}{\sigma_g \sin \alpha} \tag{27}$$

where the Dischinger effect is accounted for by the parameter

$$a = a(\zeta) = \frac{\gamma^2 E H^2}{12\sigma_g^3 (\zeta)} \tag{28}$$

which defines the stays' deformability.
   If, as usually happens, tension σ_g produced in the stays by the dead load is unchanged stay by stay, parameter a becomes constant.
   We will assume from now onwards that stays' design is such that σ_g is constant. Equation (26) may thus be written as

$$\frac{I}{H^3} \frac{\sigma_g}{g} V^{IV} + \frac{\sin^2 \alpha}{1 + a\zeta^2} V - \frac{\sin \alpha \cos \alpha}{1 + a\zeta^2} (U \mp W) = \frac{p\sigma_g}{gE} \tag{26'}$$

or

$$\frac{\epsilon^4}{4} V^{IV} + \varphi(\zeta)V - \zeta\varphi(\zeta)(U \mp W) = P(\zeta) \tag{29}$$

where

$$\frac{\epsilon^4}{4} = \frac{I\sigma_g}{H^3 g} \qquad \epsilon = \left(\frac{4I\sigma_g}{H^3 g}\right)^{1/4} \tag{30}$$

$$\frac{\sin^2 \alpha}{1 + a\zeta^2} = \frac{1}{(1 + a\zeta^2)(1 + \zeta^2)} = \varphi(\zeta) \tag{31}$$

$$\frac{\sin \alpha \cos \alpha}{1 + a\zeta^2} = \frac{\zeta}{(1 + a\zeta^2)(1 + \zeta^2)} = \zeta\varphi(\zeta) \tag{32}$$

$$P(\zeta) = \frac{p(\zeta)}{g} \frac{\sigma_g}{E}. \tag{33}$$

The two equations which give the equilibrium of the pylon top may similarly be written dimensionless so that the following set of equations is found:

Girder equilibrium

$$\frac{\epsilon^4}{4} V^{IV} + \varphi V - \zeta\varphi(U \mp W) = P \tag{34}$$

Left pylon equilibrium

$$\rho W - (\rho + \chi)U + \int_L \zeta\varphi V \, d\zeta = 0 \tag{34'}$$

Right pylon equilibrium

$$\rho W + (\rho + \chi)U - \int_R \zeta\varphi V \, d\zeta = 0 \tag{34''}$$

where

$$\rho = \int_L \frac{\cos^2 \alpha}{1 + a\zeta^2} \, d\zeta + \chi_0 \tag{35}$$

$$\chi_0 = \frac{E_0^* A_0}{E} \frac{\sigma_g}{gH} \sin \alpha_0 \cos^2 \alpha_0 \tag{36}$$

$$\chi = \frac{K\sigma_g}{Eg}. \tag{37}$$

The exact solution of eqns (34) is usually quite difficult to find. An approximate solution may be found, however, observing that:
(i) the bridge's statical behaviour is always characterized by a "truss-like" effect, which usually prevails over the girder's bending. We may actually suppose axial forces in the bridge to be well defined on the truss-structure scheme (namely girder inertia $I = 0$), while the flexural effects are, on the contrary, of a local nature.
(ii) Parameter ϵ found in eqn (30) is of main importance to the solution of eqns (34) and may be written as

$$\epsilon = \left[\frac{4I/H^4}{g/\sigma_g H}\right]^{1/4}, \tag{30'}$$

that is, as the ratio between girder stiffness I/H^4 and stay stiffness $g/\sigma_g H$. Actually, since the ratio H/L is usually constant, parameter I/H^4 is also proportional to I/L^4 and can thus be taken as a measure of girder stiffness. Parameter $g/\sigma_g H$ is instead essentially proportional to the cross-sectional area of stays, and the ratio (30') may therefore be regarded as a measure of the stiffness between deck and stays.

It may immediately be seen that the value of ϵ in long-span bridges is small, usually about $0.1 \div 0.3$.

Both observation (i) and (ii) are therefore strictly related: that is, the assumption of a truss-like behaviour in cable-stayed bridges is connected to the value of ϵ: the smaller the values of ϵ, the more truss-like the bridge's behaviour.

These observations will be used and fully proven by the approximate solution of the set of eqns (34) we shall give below.

3.2 The truss solution and the secondary girder bending

Given the load distribution $P(\zeta)$, let $\mathbf{u}(\zeta)$ (V, U, W) be the general solution of the equilibrium equations:

$$\mathbf{u}(\zeta) = \mathbf{u}_0(\zeta) + \mathbf{u}_1(\zeta) \tag{38}$$

where $\mathbf{u}_1$ is the general solution of the homogeneous equation, and $\mathbf{u}_0$ is a particular one.

Approximate solution $\mathbf{u}_0$ and $\mathbf{u}_1$ can be found supposing parameter ϵ in (34) to be conveniently small.

Since ϵ relates the girder flexural stiffness to the stay's extensional one, evidently the condition $\epsilon \to 0$ characterizes the structure's dominant truss behaviour. We should also notice that ϵ diminishes as the bridge's span grows so that the suggested scheme applies mainly to long spans.

Evaluation of $\mathbf{u}_0$

A particular solution of eqns (34–34'') is found noticing that displacements V_0, U_0 and W_0 in eqn (34) must be of the same magnitude as P. We may therefore neglect the quantity $\epsilon^4/4V^{IV}$; i.e. we find $\mathbf{u}_0$ on the truss-like scheme.

The set of equations in V_0, U_0 and W_0 finally reduces to

$$\varphi(\zeta)V_0 - (U_0 \mp W_0)\zeta\varphi(\zeta) = P(\zeta)$$

$$\rho W_0 - (\rho + \chi)U_0 + \int_L \zeta\varphi V_0 \, d\zeta = 0 \tag{39}$$

$$\rho W_0 + (\rho + \chi)U_0 - \int_R \zeta\varphi V_0 \, d\zeta = 0$$

which may be explicitly solved to give V_0, U_0 and W_0 directly as a function of $P(\zeta)$. After a little manipulation we get

$$W_0 = \frac{1}{2\chi_0}\left[- \int_L \zeta P \, d\zeta + \int_R \zeta P \, d\zeta \right]$$

$$U_0 = \frac{1}{2(\chi_0 + \chi)}\left[+ \int_L \zeta P \, d\zeta + \int_R \zeta P \, d\zeta \right] \tag{40}$$

$$V_0 = (U_0 \mp W_0)\zeta + \frac{P(\zeta)}{\varphi(\zeta)}.$$

We notice that, since the load $P(\zeta)$ may be an arbitrary function, the solution $u_0(\zeta)$ may show some discontinuities which make it not compatible. In such a case the general solution $u_1(\zeta)$ of the homogeneous problem will provide the compatibility of the complete solution.

Evaluation of displacements u_1

An approximate solution of the homogeneous system is found by choosing expressions of $V_1(\zeta)$ similar to the solution of the scheme of a beam on elastic soil. More specifically, solutions of the type

$$V_1(\zeta) = e^{f(\zeta)} \sin f(\zeta) \tag{41}$$

will be studied where $f(\zeta)$ is an appropriate function.

Extensively speaking, we shall examine the four damped sinusoidal functions defined as

$$V_1(\zeta) = e^{(\pm 1 \pm i)f(\zeta)} \tag{42}$$

which, if $f(\zeta) = \lambda\zeta$, are the four independent solutions of the problem of the Winkler beam.

We show now that if $f(\zeta)$ is taken so that

$$f(\zeta) = \frac{1}{\epsilon} \int_0^\zeta \varphi^{1/4} \, d\zeta, \tag{43}$$

and setting

$$U_1 = W_1 = 0, \tag{44}$$

we get approximate solutions (which apply as $\epsilon \to 0$) of the homogeneous problem described by the set of equations:

$$\frac{\epsilon^4}{4} V_1^{IV} + \varphi V_1 - (U_1 \mp W_1)\zeta\varphi = 0 \tag{45'}$$

$$\rho W_1 - (\rho + \chi)U_1 + \int_L \zeta\varphi V_1 \, d\zeta = 0 \tag{45''}$$

$$\rho W_1 + (\rho + \chi)U_1 - \int_R \zeta\varphi V_1 \, d\zeta = 0. \tag{45'''}$$

In order to show that the solution given by (42) and (44) is correct, we evaluate the quantity $\epsilon^4/4 V_1^{IV}$ and get

$$\frac{\epsilon^4}{4} V_1^{IV} = \frac{\epsilon^4}{4} e^{(\pm 1 \pm i)f(\zeta)} [-4f'^4 + 6(\pm 1 \pm i)^3 f'^2 f''$$

$$+ 3(\pm 1 \pm i)^2 f''^2 + 4(\pm 1 \pm i)^2 f''' f' + (\pm 1 \pm i)f^{IV}]$$

and, making use of (43):

$$\frac{\epsilon^4}{4} V_1^{IV} = e^{(\pm 1 \pm i)f(\zeta)} [-\varphi(\zeta) + 0(\epsilon)]. \tag{46}$$

Let us now evaluate the integral $\int \zeta\varphi V_1 \, d\zeta$:

$$\int_L \zeta\varphi V_1 \, d\zeta = \int_L (\epsilon\zeta\varphi^{3/4}) \left(\frac{\varphi^{1/4}}{\epsilon} e^{(\pm 1 \pm i)f(\zeta)} \right) d\zeta$$

$$= \int_L (\epsilon\zeta\varphi^{3/4}) \frac{(e^{(\pm 1 \pm i)f})'}{\pm 1 \pm i} \, d\zeta \tag{47}$$

$$= \left| \epsilon\zeta\varphi^{3/4} \frac{e^{(\pm 1 \pm i)f}}{\pm 1 \pm i} \right|_{l/H}^{L/2H} - \epsilon \int_L (\zeta\varphi^{3/4})' \frac{e^{(\pm 1 \pm i)f}}{\pm 1 \pm i} \, d\zeta = 0(\epsilon).$$

We see from (47) that the integrals in both (45″) and (45‴) are of the same magnitude as ϵ. We thus deduce that U_1 and W_1 are also of the same magnitude as ϵ and may, therefore, be neglected compared to girder flexural displacements $V_1(\zeta)$ given by (42).

If we now examine the girder's equilibrium equation (45′) and recall (46) and (47) we get

$$-\varphi e^{(\pm 1 \pm i)f} + \varphi e^{(\pm 1 \pm i)f} + 0(\epsilon) = 0.$$

We thus conclude that this equation is also satisfied at least of terms of order ϵ.

In conclusion, the general solution of the homogeneous problem can be expressed as

$$U_1 = W_1 = 0$$

$$V_1(\zeta) = c_1 e^{-f(\zeta)} \sin f(\zeta) + c_2 e^{-f(\zeta)} \cos f(\zeta) + c_3 e^{f(\zeta)} \sin f(\zeta) + c_4 e^{f(\zeta)} \cos f(\zeta). \quad (48)$$

The approximate solution given by (40) and (48) reflects the truss-like behaviour of the bridge scheme we are examining; in fact the displacements given by eqn (40) correspond to $\epsilon = 0$, i.e. to the scheme with hinged connections of the stays to the girder, and therefore u_0 may be understood as a truss behaviour solution. To the term V_0, the quantity V_1 should be added. V_1 strictly depends on the parameter ϵ and represents the additional displacements required to re-establish the flexural compatibility uncomplied with by the truss solution. Overall displacements are therefore the sum of the truss solution u_0 involving the whole structure, and of the flexural share V_1, which characterizes only a local effect, since it is given by damped sinusoidal functions where damping is quicker, the smaller the value of ϵ.

The truss-like behaviour of this scheme of cable-stayed bridge has thus been analytically confirmed, behaviour being more evident, the smaller the value of ϵ, as for instance occurs as the bridge's span grows.

The wave length λ of the sinusoidal waves $V_1(\zeta)$ will be approximately evaluated so that the general solution's damped nature may be better defined.

This length varies along the deck and, at the abscissa ζ_0, is found to be such that

$$\frac{1}{\epsilon} \int_{\zeta_0}^{\zeta_0 + \lambda} \varphi^{1/4} \, d\zeta = 2\pi. \quad (49)$$

Supposing a small $\lambda(\zeta_0)$, we may write

$$\frac{1}{\epsilon} \varphi^{1/4} (\zeta_0)\lambda \cong 2\pi$$

and hence

$$\lambda(\zeta_0) \cong \frac{2\pi}{\varphi^{\frac{1}{4}}(\zeta_0)} \epsilon. \quad (50)$$

Recalling that

$$\varphi(\zeta) = \frac{1}{(1 + a\zeta^2)(1 + \zeta^2)}$$

the maximum wave length is found at the bridge's midspan, and setting $a \cong 0.05$, $L/2H \cong 2.5$ $\varphi(L/2H) \cong 0.1$, it is found to be

$$\lambda \left(\frac{L}{2H}\right) \cong 11\epsilon$$

or, being $\epsilon \cong 0.2$

$$\lambda\left(\frac{L}{2H}\right) \cong 2.2$$

while when $\zeta = 0$ we get $\varphi(0) = 1$, $\lambda(0) = 6.3\epsilon$ and, with $\epsilon \cong 0.2$, $\lambda(0) \cong 1.26$.
Now we give an approximate form of the function

$$f(\zeta) = \frac{1}{\epsilon} \int_{\zeta_0}^{\zeta} \varphi^{1/4} \, d\zeta.$$

Approximating $\varphi(\zeta)$ with

$$\varphi(\zeta) \cong (1 - b\zeta)^4 \tag{51}$$

where

$$b = \frac{1}{2} - \frac{1}{2[5(1 + 4a)]^{1/4}} \tag{52}$$

obtained by interpolating $\varphi(\zeta)$ at $\zeta = 0$ and $\zeta = 2$, and which applies for values of $a \cong 0.05 - 0.3$, we get

$$f(\zeta) = \frac{1}{\epsilon} \int_{\zeta_0}^{\zeta} \varphi^{1/4} \, d\zeta = \frac{1}{\epsilon}\left[(\zeta - \zeta_0) - \frac{b}{2}(\zeta^2 - \zeta_0^2)\right]. \tag{53}$$

3.2 *Torsion*

In this section we examine torsional effects due to load eccentricities. Since stays respond differently to positive or negative stress increments, torsion and vertical bending of the girder are coupled in a nonlinear analysis. However, if the tangent Dischinger response of the stays is assumed, flexural and torsional effects may be examined separately. We also assume that the girder is symmetric with respect to a vertical longitudinal plane, and we consider the two possibilities of Fig. 5, that is *H*-shaped and *A*-shaped towers. Within these assumptions the bridge's torsional deformation is defined by the torsional rotation $\theta(z)$ of the girder and by the rotations ψ_L and ψ_R of the tower tops sections (Fig. 6).

For *A*-shaped towers it can be used $\psi_L = \psi_R = 0$.

The torsional equilibrium equation of the girder can be written in the form

$$C_t\theta'' = -(m_s + m_t) \tag{54}$$

where C_t is the torsional girder stiffness, m_t the distributed torsional couple due to the external load, and m_s the torsional action on the girder produced by the stay's curtains.
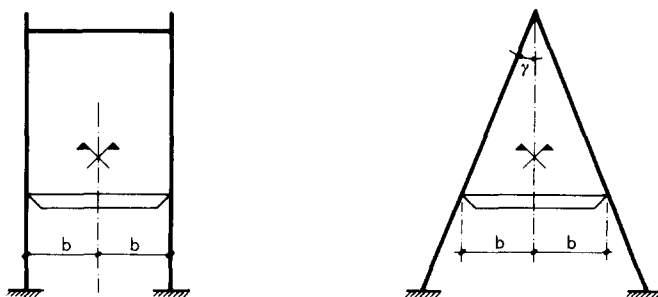

Fig. 5. (a) H-shaped tower, (b) A-shaped tower.

As in the previous section, it is possible to express the stay's action as a function of the bridge deformation parameters $\theta(z)$, ψ_L, ψ_R. With reference to the left half of the bridge we therefore get the following equilibrium equations, written in dimensionless form:

Girder equilibrium

$$\tau^2\theta'' - \varphi(\zeta)\theta + \frac{\zeta\varphi(\zeta)}{\rho + \chi} \int_L \theta(\zeta)\zeta\varphi(\zeta)\,d\zeta = -\mu \tag{55}$$

Left tower equilibrium

$$\psi_L = \frac{1}{\rho + \chi} \int_L \theta(\zeta)\zeta\varphi(\zeta)\,d\zeta \tag{56}$$

where

$$(\ )' = \frac{d(\ )}{d\zeta} \qquad \tau^2 = \frac{C_t\sigma_g}{Eb^2Hg} \qquad \mu(\zeta) = \frac{H\sigma_g}{Eb^2g}\,m_t(\zeta) \tag{57}$$

and the other quantities are as previously defined by eqns (31), (32), (35)–(37).

The case of A-shaped towers can be obtained from eqn (55), by assuming that the anchor cable is infinitely stiff so that the rotation ψ_L of the tower becomes zero. In this case, therefore, we put $\chi_0 = \infty$ in eqns (55) and (56).

An approximate solution of eqn (55) can now be found with the same procedure used in Section 3.2. For long-span bridges, in fact, the parameter τ is usually small. Then a particular solution θ_0, $(\psi_L)_0$ of eqns (55), (56) is evaluated on the truss-like scheme; with $\tau = 0$, we get from eqns (55), (56)

$$\theta_0(\zeta) = \frac{\mu}{\varphi(\zeta)} + \frac{1}{\chi + \chi_0}\,\zeta \int_L \mu(\zeta)\zeta\,d\zeta \tag{58}$$

$$(\psi_L)_0 = \frac{1}{\rho + \chi} \int_L \theta_0(\zeta)\zeta\varphi(\zeta)\,d\zeta. \tag{59}$$

As in Section 3.2 it is possible to prove that, neglecting quantities of order τ in eqn (55), the complete expression of the girder rotation is

$$\theta(\zeta) = C_1 e^{f(\zeta)} + C_2 e^{-f(\zeta)} + \theta_0(\zeta) \tag{60}$$

and

$$\psi_L = (\psi_L)_0 \tag{61}$$

where

$$f(\zeta) = \frac{1}{\tau} \int_{\zeta_0}^{\zeta} \varphi^{1/2}(\zeta)\,d\zeta. \tag{62}$$

4. APPLICATIONS

The approximate solutions given in the previous sections can be quite easily applied to give simple expressions of the effects produced by live loads. As an illustration, the bridge's midspan cross section will be analyzed and its maximum deflection and positive bending moment evaluated. Furthermore, the effect of a uniform eccentric load is considered.

4.1. *Evaluation of maximum midspan deflection*

Maximum midspan deflection occurs when the whole main span is under a live load. The load condition is uniform throughout the main span.

Taking the symmetry of the load condition into account, W_0, U_0 and V_0 are expressed as follows:

$$W_0 = 0$$

$$U_0 = \frac{P}{\chi_0 + \chi} \int_0^{L/2H} \zeta \, d\zeta = \frac{1}{2} \left(\frac{L}{2H}\right)^2 \frac{P}{\chi_0 + \chi} \tag{63}$$

$$V_0(\zeta) = P\left[\frac{1}{2}\left(\frac{L}{2H}\right)^2 \frac{1}{\chi_0 + \chi} \zeta + (1 + a\zeta^2)(1 + \zeta^2)\right].$$

In order to find the complete solution at the bridge's middle part, the solution of the homogeneous problem, in the middle part, is taken in the form

$$V_1(\zeta) = c_1 e^{-f(\zeta)} \sin f(\zeta) + c_2 e^{-f(\zeta)} \cos f(\zeta) \tag{64}$$

where

$$f(\zeta) = \frac{1}{\epsilon} \int_\zeta^{L/2H} \varphi^{1/4} \, d\zeta. \tag{65}$$

This solution represents the flexural waves decreasing from the midspan towards the towers.

Finally deflection $V(\zeta)$ is found as

$$V(\zeta) = P\left[\frac{1}{2}\left(\frac{L}{2H}\right)^2 \frac{1}{\chi_0 + \chi} \zeta + (1 + a\zeta^2)(1 + \zeta^2)\right]$$

$$+ P\frac{\epsilon}{2\varphi^{1/4}}\left[\frac{1}{2}\left(\frac{L}{2H}\right)^2 \frac{1}{\chi_0 + \chi} + 2(1 + a)\frac{L}{2H} + 4a\left(\frac{L}{2H}\right)^3\right]$$

$$\cdot [e^{-f(\zeta)} \sin f(\zeta) - e^{-f(\zeta)} \cos f(\zeta)]. \tag{66}$$

If, for instance, $\zeta = L/2H$, the maximum midspan deflection is found to be

$$V\left(\frac{L}{2H}\right) = P\left[\frac{1}{2}\left(\frac{L}{2H}\right)^3 \frac{1}{\chi_0 + \chi} + \left(1 + a\left(\frac{L}{2H}\right)^2\right)\left(1 + \left(\frac{L}{2H}\right)^2\right)\right]$$

$$- P\frac{\epsilon}{\varphi^{1/4}}\left[\frac{1}{4}\left(\frac{L}{2H}\right)^2 \frac{1}{\chi_0 + \chi} + (1 + a)\frac{L}{2H} + 2a\left(\frac{L}{2H}\right)^3\right]. \tag{67}$$

We notice now that, when a uniform load is applied to the main span, stresses in the mid-bridge stays are practically proportional to the applied load and therefore:

$$\beta = \frac{\sigma_{g+p}}{\sigma_g} \cong \frac{g + p}{g}. \tag{68}$$

Furthermore, the axial force produced by dead load in the anchor stays is

$$(N_g)_0 = \frac{gl}{2}\left[1 + \left(\frac{l}{H}\right)^2\right]^{1/2}\left[\left(\frac{L}{2l}\right)^2 - 1\right]; \tag{69}$$

a live load p over the whole main span gives

$$(N_p)_0 = \frac{pl}{2}\left[1 + \left(\frac{l}{H}\right)^2\right]^{1/2}\left[\frac{L}{2l}\right]^2, \tag{70}$$

and thus for the anchor stays

$$\beta_0 = \frac{\sigma_{(g+p)}}{\sigma_g} = 1 + \frac{p}{g}\frac{\left(\frac{L}{2l}\right)^2}{\left(\frac{L}{2l}\right)^2 - 1}. \tag{71}$$

For the load conditions being examined, tensions in the stays and the anchor cable may thus be quite accurately evaluated when dead loads g and live loads p are present. In order for mid-span displacement to be evaluated from (67), it is convenient to evaluate the stays' elastic response by means of the secant modulus defined by (9) where β is given (68) and (71).

The quantity $\chi_0 + \chi$ may be expressed as

$$\chi_0 + \chi = \frac{\beta_0/\beta}{1 + \bar{a}r_2^2\dfrac{\beta_0}{\beta}\dfrac{1 + \beta_0}{1 + \beta}}\frac{1}{2}r_2^3(1 + r_2^2)^{-1}\left(\frac{r_1^2}{r_2^2} - 1\right) + \frac{K}{g}\frac{\sigma_a}{E}\frac{1}{1 + \dfrac{p}{g}} \tag{72}$$

where σ_a is the allowable stress in the stays and

$$\bar{a} = \frac{\gamma^2 E H^2}{12\sigma_g^3}\frac{1 + \beta}{2\beta^2} = a\frac{1 + \beta}{2\beta^2} \tag{73}$$

$$r_1 = L/2H$$

$$r_2 = l/H.$$

Concluding, the maximum midspan deflection δ, referred to span L, is given by

$$\frac{\delta}{L} = \frac{p}{g}\frac{\sigma_a}{E}\frac{1}{1 + \dfrac{p}{g}}\frac{1}{2r_1}\left\{\frac{1}{2}r_1^3\frac{1}{\chi_0 + \chi} + (1 + \bar{a}r_1^2)(1 + r_1^2)\right.$$

$$\left. - \epsilon(1 + \bar{a}r_1^2)^{1/4}\left(\frac{1}{4}r_1^2\frac{1}{\chi_0 + \chi} + (1 + \bar{a})r_1 + 2\bar{a}r_1^3)(1 + r_1^2)^{1/4}\right\}, \tag{74}$$

where $\chi_0 + \chi$ is given by (72).

The parameters involved are, therefore,

$$r_1 - r_2 - \frac{\sigma_a}{E} - \frac{k}{g} - a - \epsilon - \frac{p}{g},$$

of which the first three may be regarded as fixed and the fourth, of little influence, is averaged as 50.

Actually, it is enough to study the influence of a and p/g, when making a qualitative investigation of the bridge's mid-span deformability.

The dependence of the ratio δ/L on the a and ϵ parameters is plotted in Fig. 7 where the usual value $p/g = 1$ has been assumed.

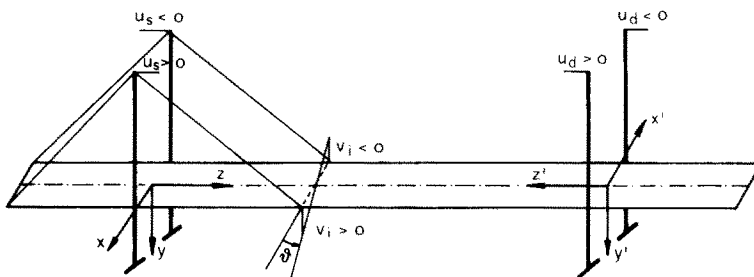The first thing to notice is that δ/L depends almost linearly on a.

Fig. 6. Torsional deformation parameters.

Similarly, δ/L linearly depends on ϵ and it is still quite proportional to p/g for usual values of such a parameter. These results allow us to make the following comments.

Firstly, midspan deflections linearly grow with the product $a \cdot L$, and therefore with L^3, assuming that, given $L/2H$ and σ_g, a is proportional to L^2.

The influence of ϵ on deflections is not relevant and decreases as the span grows. The girder's moment of inertia thus cannot be taken as a meaningful parameter, which may help in restricting the bridge's deformability as the span grows.

In Fig. 7 a comparison is also made among the results given by formula (74) and by some numerical computations using a finite element analysis of eqns (34). The comparison shows good agreement, especially for ϵ less than 0.2.

4.2. *Evaluation of maximum midspan positive bending moment*

The maximum bending moment is evaluated by means of the corresponding influence line. Using the solution (41) we get

$$V(\zeta) = \frac{\zeta}{\chi_0 + \chi} \frac{\epsilon^3}{8} \varphi^{1/4} \left(\frac{L}{2H}\right) - \frac{1}{4} \frac{\epsilon}{\varphi^{1/4}} [e^{-f(\zeta)} - e^{-f(\zeta)} \cos f(\zeta)]. \tag{75}$$
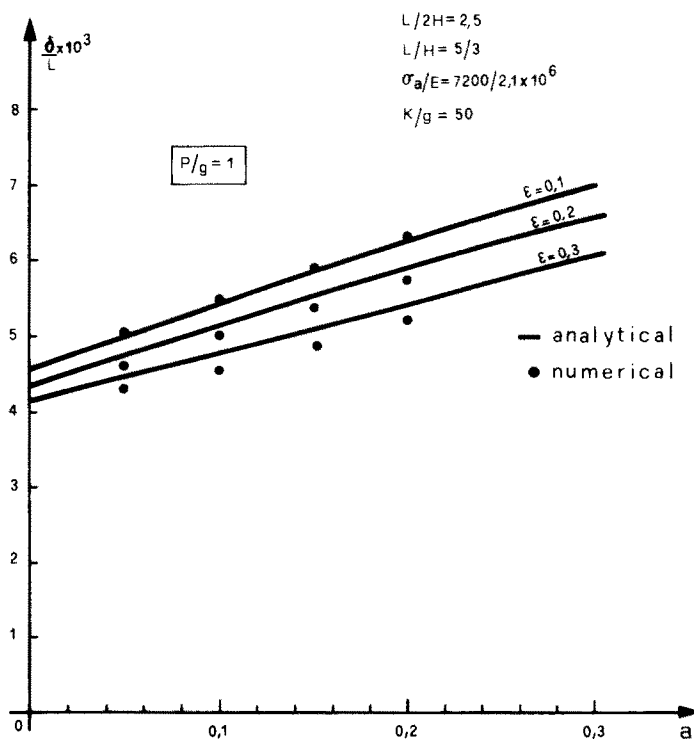

Fig. 7. Maximum midspan deflection as function of $a = \gamma^2 E H^2 / 12 \sigma_g^3$.

The magnitude of the first term of (75) is ϵ^3 and may therefore be neglected compared to the second. Maximum bending moment is then evaluated taking the following expression of the influence line:

$$V(\zeta) \cong -\frac{1}{4} \frac{\epsilon}{\varphi^{1/4}} [e^{-f(\zeta)} \sin f(\zeta) - e^{-f(\zeta)} \cos f(\zeta)]. \tag{76}$$

The function $f(\zeta)$ changes sign when ζ is such that

$$\sin f(\zeta) = \cos f(\zeta) = \sqrt{2}/2 \tag{77}$$

and thus

$$f(\bar{\zeta}) = \frac{\pi}{4}. \tag{78}$$

Taking expression (53) of $f(\zeta)$ we get

$$\bar{\zeta} = \frac{1}{b} - \frac{1}{b}\left[\left(1 - b\frac{L}{2H}\right)^2 + 2b\frac{\pi}{4}\epsilon\right]^{1/2}. \tag{79}$$

The dimensionless maximum moment is, therefore:

$$m_{\text{max}} = 2P \int_{\bar{\zeta}}^{L/2H} V(\zeta)\, d\zeta \tag{80}$$

and since between $\bar{\zeta}$ and $L/2H$ the influence line is practically linear, the integration of (80) is approximated as follows:

$$m_{\text{max}} = 2P \frac{1}{2} V\left(\frac{L}{2H}\right)\left(\frac{L}{2H} - \bar{\zeta}\right); \tag{81}$$

considering that $f(L/2H) = 0$, we have

$$m_{\text{max}} = P \frac{\epsilon}{4\varphi^{1/4}} \left(\frac{L}{2H} - \bar{\zeta}\right) \tag{82}$$

and in a dimensional form

$$M_{\text{max}} = pH^2 \frac{\epsilon}{4\varphi^{1/4}} \left(\frac{L}{2H} - \bar{\zeta}\right). \tag{83}$$

The values of M_{max}/pH^2 are plotted in Fig. 8 as functions of the a and ϵ parameters. Also in this case the comparison with the numerical results is satisfying for $\epsilon \leq 0.2$.

4.3. *Torsional effect*
The previously found results will now be applied to evaluate the effect of a uniform torsional load:

$$\mu(\zeta) = \mu_0. \tag{84}$$

This loading condition is interesting because in such a case the maximum rotation at midspan ($\zeta = L/2H$), and the maximum torque of the girder at $\zeta = 0$ occur.
The symmetry of the structural scheme gives

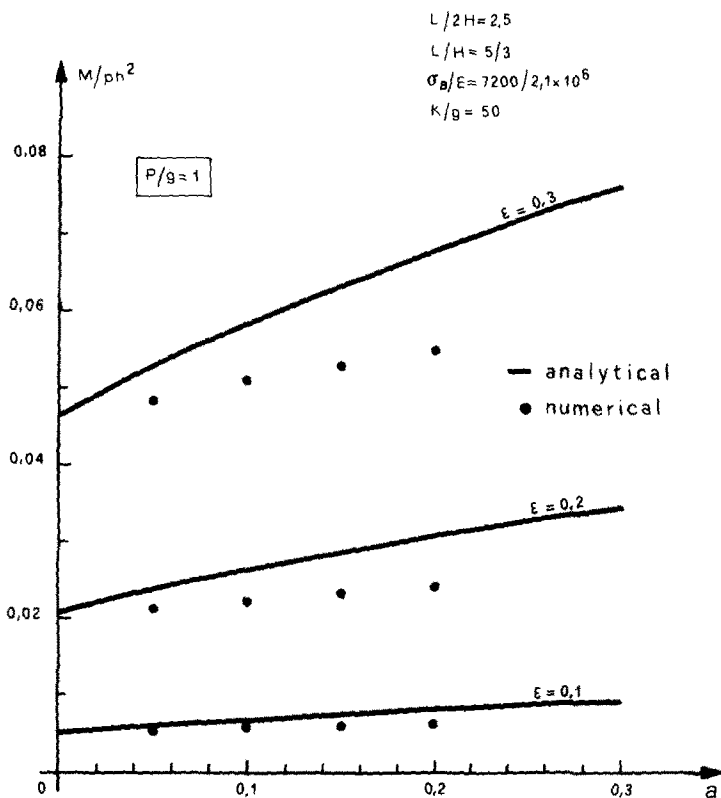$$\psi_L = -\psi_R = \psi. \tag{85}$$

Fig. 8. Maximum midspan bending moment as function of $a = \gamma^2 EH^2/12\sigma_v^3$.

From eqns (58), (59) we get

$$\vartheta_0 = \frac{\mu_0}{\varphi} + \frac{1}{2}\frac{\mu_0}{\chi_0 + \chi}\left(\frac{L}{2H}\right)^2 \zeta \tag{86}$$

$$\psi = \frac{1}{2}\frac{\mu_0}{\chi_0 + \chi}\left(\frac{L}{2H}\right)^2. \tag{87}$$

If the boundary conditions are

$$\theta'\left(\frac{L}{2H}\right) = 0 \tag{88}$$

$$\theta(0) = 0 \tag{89}$$

we get from eqn (60) the following expression of the complete solution $\theta(\zeta)$:

$$\vartheta(\zeta) = \mu_0 \left\{ \frac{1}{\varphi(\zeta)} + \frac{1}{2}\frac{\zeta}{\chi + \chi_0}\left(\frac{L}{2H}\right)^2 - \frac{\tau}{\varphi^{1/2}(L/2H)}\left[\left(\frac{1}{\varphi}\right)'_{L/2H} \right.\right.$$

$$\left.\left. + \frac{1}{2}\frac{1}{\chi + \chi_0}\left(\frac{L}{2H}\right)^2\right] \cdot e^{-f(\zeta)} - \frac{1}{\varphi(0)}e^{-f\left(\frac{L}{2H} - \zeta\right)} \right\} \tag{90}$$

Therefore the maximum rotation at midspan is

$$\vartheta\left(\frac{L}{2H}\right) \approx \mu_0 \left\{ \frac{1}{\varphi(L/2H)} + \frac{1}{2}\frac{1}{\chi + \chi_0}\left(\frac{L}{2H}\right)^3 - \frac{\tau}{\varphi^{1/2}(L/2H)} \right.$$

$$\left. \cdot \left[\left(\frac{1}{\varphi}\right)'_{L/2H} + \frac{1}{2}\frac{1}{\chi + \chi_0}\left(\frac{L}{2H}\right)^2\right] \right\} \tag{91}$$
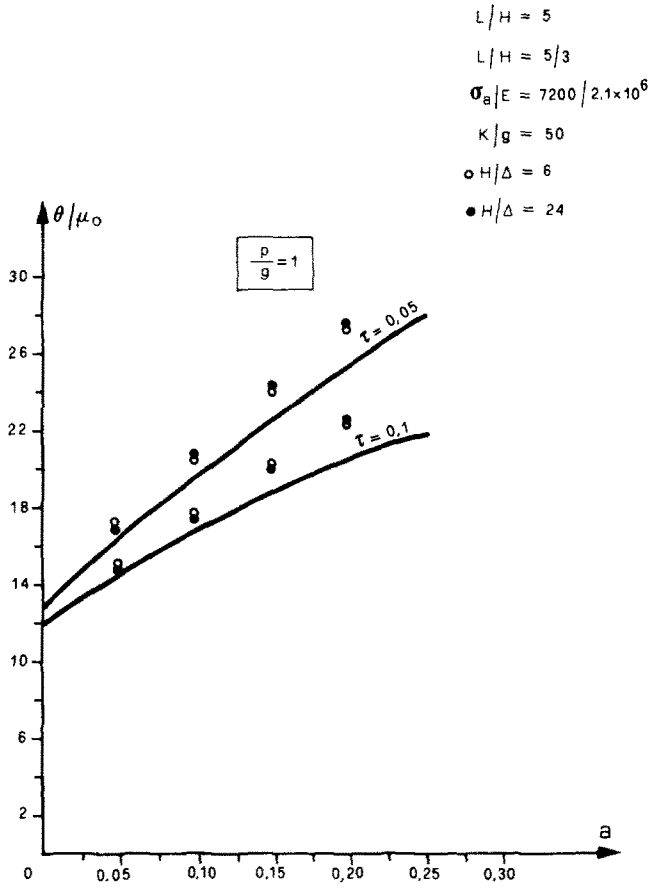
Fig. 9. Maximum midspan torsional rotation as function of $a = \gamma^2 EH^2/12\sigma_g^3$.

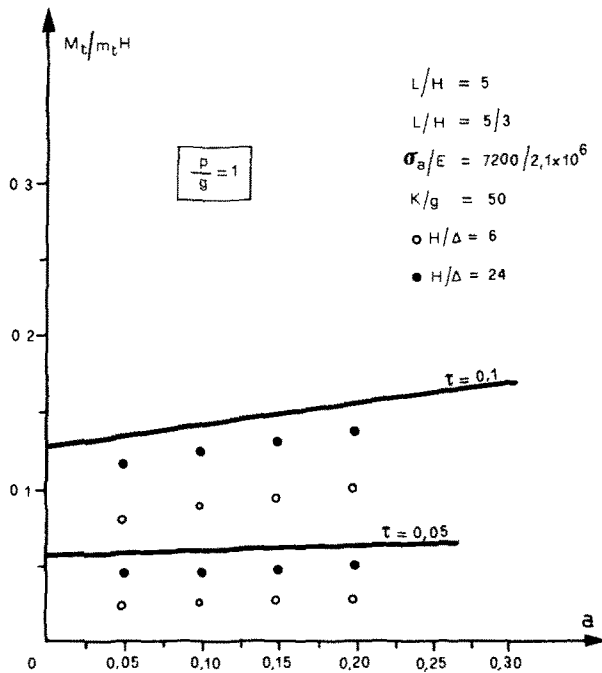Fig. 10. Maximum twisting moment at sections $\zeta = 0$ as function of $a = \gamma^2 EH^2/12\sigma_g^3$

and the twisting moment at the Section $\zeta = 0$:

$$M_t(0) = \frac{C_t}{H} \mu_0 \left[\frac{1}{2} \frac{1}{\chi + \chi_0} \left(\frac{L}{2H} \right)^2 + \frac{1}{\tau} \right]$$

$$\frac{M_t(0)}{m_t H} \cong \left[\tau + \tau^2 \frac{1}{2} \frac{1}{\chi + \chi_0} \left(\frac{L}{2H} \right)^2 \right].$$

Quantities

$$\vartheta \left(\frac{L}{2H} \right), \qquad \frac{M_t(0)}{m_t H}$$

are shown in Figs. 9 and 10 for typical values of the parameters:

$$r_1, r_2, \frac{\sigma_a}{E}, \qquad \frac{K}{g}, \qquad a, \tau, \qquad \frac{p}{g}$$

Figures 9 and 10 also show the results of the numerical analysis.

5. CONCLUSIONS

The static behaviour of long-span cable-stayed bridges has been analyzed by means of a continuous model. Simple expressions have been derived of the main effects produced by live loads. The obtained results collect the main qualitative aspects of the bridge behaviour.

The comparison with numerical solutions shows that the proposed continuous model usually gives conservative results as, for instance, in the case of maximum midspan deflection and bending moment evaluation.

REFERENCES

1. F. Leonhardt and W. Zellner, *Cable-Stayed Bridges: Report on Latest Developments*, Canadian Structural Engineering Conference, Toronto (1970).
2. F. Leonhardt and W. Zellner, *Comparative Investigations Between Suspension Bridges and Cable-Stayed Bridges for Span Exceeding 600 m*, IABSE Publication 32-1 (1972).
3. F. Leonhardt, *Cable-Stayed Bridges*, IABSE Surveys, S-13/80 (1980).
4. F. De Miranda, *Il ponte strallato: soluzione attuale del problema delle grandi luci*, Costruzioni Metalliche, Vol. 1 (1971).
5. W. Podolny and J. B. Scalzi, *Construction and Design of Cable-Stayed Bridges*, John Wiley & Sons, New York (1976).
6. M. S. Troitsky, *Cable-Stayed Bridges*, Crosby Lockwood Staples, London (1977).
7. F. De Miranda, A. Grimaldi, F. Maceri and M. Como, *Basic Problems in Long-span Cable-Stayed Bridges*, Department of Structures, University of Calabria, Report no. 25 (1979).